

Two Dimensional Electrons in (100) Oriented Silicon Field Effect Structures in the Region of Low Concentrations and High Mobilities

V. T. Dolgoplov¹

¹*Institute of Solid State Physics, Russian Academy of Sciences,
Chernogolovka, Moscow region, 142432 Russia, e-mail: dolgop@issp.ac.ru*

A comparative analysis of experimental data on electron transport in Si (100) MOSFETs in the region of high mobilities and strong electron-electron interaction is carried out. It is shown that electrons can be described by the model of a noninteracting gas with the renormalized mass and Lande factor, which allows experimentally verifiable predictions.

PACS numbers:

Although the experimental studies of the two-dimensional electron gas in silicon field-effect structures already have a history of more than half a century¹, they still go on (see, e.g.,²⁻⁴). Interest in this field of research is mainly related to the possible metal-insulator transition⁵, as well as the manifestations of strong electron-electron interaction^{2-4,9-11} for the lowest attainable electron densities on the order of 10^{11} cm^{-2} . In this range of electron densities, the effect of electron-electron interaction cannot be described in terms of a perturbation theory series, because the expansion parameter r_s is considerably larger than unity. Therefore, experimental results should be interpreted very cautiously and, in the first place, one needs to identify the common features revealed in experiments on samples from different manufacturers by different research groups using different methods of experimental data treatment. In this publication, a part of this program is performed and some further experiments are suggested.

Almost noninteracting quasiparticles carrying a unit charge exist only very close to the Fermi energy. For them, one can define the Fermi momentum p_F , determined by the number of free electrons introduced into the originally neutral system; the velocity v_F ; and the Lande factor g^* , which characterizes only the quasiparticles at the Fermi surface. Each of these quantities can be measured experimentally.

The most convenient and accurate experimental method to find the relation between the Fermi momentum and Fermi velocity is to determine the electron effective mass $m = p_F/v_F$ from the analysis of the temperature dependence of the amplitude and shape of the Shubnikov-de Haas oscillations. It is appropriate to begin the analysis of experimental results with measurements of this kind. However, it is necessary to take into account a number of factors that compel one to treat with some caution even these most reliable data. (i) The amplitude of quantum oscillations needs to be sufficiently small both because of the limitation on the validity of the Lifshitz-Kosevich formula and because of the possible strong nonparabolicity of the spectrum¹² in the vicinity of the Fermi level. The effective mass is overestimated owing to the first factor and underestimated owing to the second. (ii) The quantum oscillation numbers have to be sufficiently large to satisfy the assumptions made in the Lifshitz-Kosevich theory. (iii) The quantum relaxation time has to be independent of the temperature. Otherwise, the effective mass will be overestimated or underestimated, depending on the temperature range⁴.

Raw experimental data on the measurements of the effective mass can be found in¹³ and¹⁴. These measurements were carried out by different experimental groups and, furthermore, were performed on silicon field-effect structures made by different manufacturers. According to^{4,10}, the experimental data obtained for the effective mass can be well described by the interpolation formula

$$m = 0.205m_e(1 + 0.035r_s + 0.00016r_s^4) \quad (1)$$

in the range $8 > r_s > 1.5$, where $r_s = 2.63(10/n_s)^{1/2}$ and the electron density is measured in units of 10^{11} cm^{-2} .

Figure 1 shows the dependence of the effective mass on the electron density as a plot of $m_b n_s / m$ versus n_s , where $m_b = 0.19m_e$ is the band effective mass. The thick solid line corresponds to the effective mass given by Eq.(1), and points represent the experimental data from¹⁴. In the range of electron densities where measurements were carried out, both sets of experimental data can be very well described by the dependence

$$m = m_b \frac{n_s}{(n_s - n_c)}. \quad (2)$$

Indeed, in coordinates used in Fig.1, each of these data sets can be fitted by a straight line with a slope of 42° . This corresponds to an experimentally obtained mass m_b that is 10% smaller than that known from¹. Equation (2) describes data obtained for a large number of samples with different mobilities. It looks like the critical density n_c is determined by the interaction between electrons and depends weakly on the chaotic potential.

A behavior described by Eq.(2) in the vicinity of the quantum phase transition point in a strongly interacting two-dimensional electron system was predicted in a number of publications¹⁵⁻¹⁸. Note that Eq.(2) remains valid up to electron densities as high as at least 10^{12} cm^{-2} .

The extrapolated values of the critical electron density are somewhat different: $n_{c1} = 0.54 * 10^{11} \text{ cm}^{-2}$ and $n_{c2} = 0.64 * 10^{11} \text{ cm}^{-2}$. Most probably, the 15 % discrepancy occurs for purely technical reasons such as different methods of experimental data treatment and the overestimation of the experimental accuracy. Certainly, the importance of more fundamental factors, for example, the different widths of the depletion layer in samples supplied by different manufacturers and,

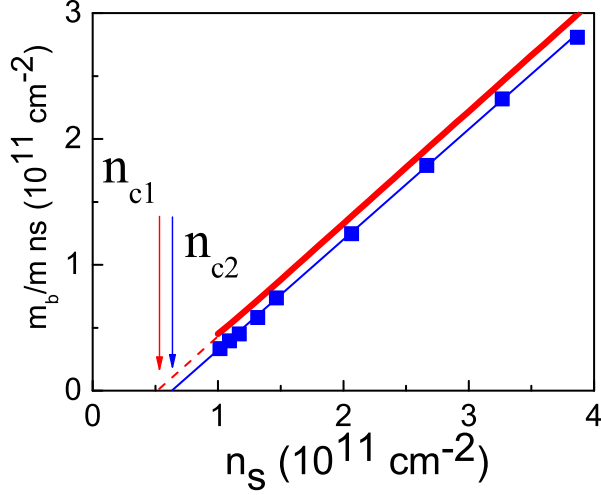


FIG. 1: (Color online) Reciprocal effective mass versus the electron density. The vertical axis is chosen so that the corresponding dependence for a system of noninteracting electrons is a straight line with a slope of 45° passing through the origin. The thick solid line corresponds to the experimental results fitted by Eq. (1). Symbols and the straight line drawn through them represent the data from [14]. Arrows show the critical densities arising upon the linear extrapolation of the experimental data.

as a consequence, the difference in the Coulomb interaction energy or the degree of disorder, cannot be excluded.

Another reliably established fact is the independence of the effective mass of electrons in Si (100) MOSFETs on the degree of spin polarization of the electron system. This result was first obtained from the analysis of the temperature dependence of the Shubnikov-de Haas oscillations in the presence of a magnetic field component parallel to the interface¹⁴ and recently confirmed (at least, to the first approximation) by independent experiments⁴. This conclusion is also supported by some of the raw experimental data presented in earlier publication¹³ and by calculations for a multivalley electron system in the limiting case of weak interaction¹⁹.

The further interpretation of the experimental data requires additional assumptions that are, generally speaking, poorly justified. Let us assume that a system of strongly interacting particles can be described in terms of a Fermi gas of noninteracting quasiparticles with the same parameters as those at the Fermi level, which depend only on the electron density. Indirectly, this assumption is supported by a quantum Monte Carlo calculation, which indicated that the difference between the energies of a spin-polarized and a spin-unpolarized electron system is proportional to the square of the degree of polarization, similarly to the case of free electrons²⁰. In addition, let us extrapolate the linear dependence in Fig.1 to the intersection with the horizontal axis and further along this axis to zero.

For $n_s > n_c$, the chemical potential level with respect to the bottom of the band will be equal to

$$\mu(n_s) = n_s \pi \hbar^2 / 2m = (n_s - n_c) \pi \hbar^2 / 2m_b \quad (3)$$

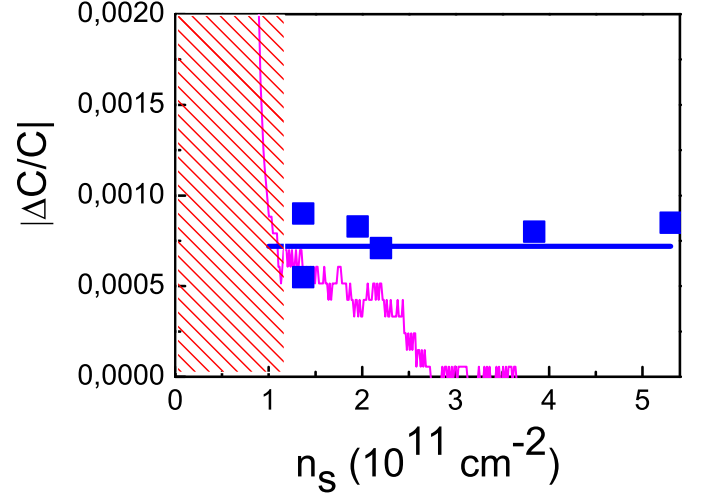


FIG. 2: (Color online) Experimentally determined change in the capacitance caused by the variation of the density of states from the value corresponding to the spin unpolarized electron system to an infinitely large value (symbols) and caused by the complete spin polarization of electrons (noisy curve, $B = 9.9$ T). The solid horizontal line shows the value expected for a gas of noninteracting electrons. The shaded part of the plot at low electron densities corresponds to the region of electron localization in a magnetic field completely spin polarizing the electron system.

According to this expression, the thermodynamic density of states $\partial n_s / \partial \mu$ in this strongly interacting electron system coincides with that in the original noninteracting electron gas: $\partial n_s / \partial \mu = 2m_b / \pi \hbar^2$. The validity of the latter relation can be tested experimentally. For this purpose, one needs to measure the difference between the MOSFET capacitances in zero magnetic field and in those quantizing magnetic fields for which the thermodynamic density of states becomes infinite (the method is described in detail, e.g., in Ref.²¹).

The results of such measurements are shown in Fig.2. One can see that, in the absence of a magnetic field, the thermodynamic density of states does coincide within the experimental error with that of noninteracting electrons, and the above assumptions lead to conclusions that agree with the experiment.

Now, let us consider the case of a magnetic field oriented parallel to the interface whose strength B is less than or equal to the field B_p required to attain the complete spin polarization. The magnetic moment M per unit area of a two dimensional electron system is determined by the density of states for a fixed number of electrons and the difference between the energies of electrons with the spin oriented along and opposite to the field:

$$M = (\mu_B g)^2 B \frac{m_b}{2\pi \hbar^2} \frac{n_s}{n_s - n_c}, \quad (4)$$

where μ_B is the Bohr magneton and g is the interaction renormalized Lande factor. It is assumed here, in the context of experimental data testifying that the effective mass is independent of the parallel component of the magnetic field, that the critical density n_c is also independent of the magnetic field.

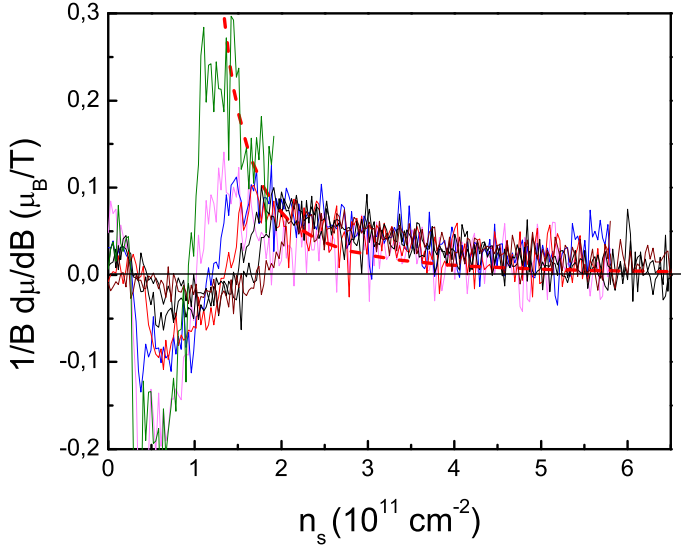


FIG. 3: (Color online) Comparison of the experimental results from [23] (for magnetic fields of 1.5, 2, 3, 4, 5, 6, and 7 T) with (dashed line) the calculation according to Eq.(6).

Using the relation

$$\frac{\partial M}{\partial n_s} = -\frac{\partial \mu}{\partial B}, \quad (5)$$

the following expression for a quantity that can be measured experimentally is obtained:

$$\frac{\partial \mu}{\partial B} = (\mu_B g)^2 B \frac{m_b}{2\pi\hbar^2} \frac{n_c}{(n_s - n_c)^2}. \quad (6)$$

It is noteworthy that Eq.(6) contains only experimentally measurable quantities g and n_c and no fitting parameters.

Experimental data on the derivative $\frac{\partial \mu}{\partial B}$ in different magnetic fields were obtained in Ref.s^{22,23}. In Fig.3, data from Ref.²³ are compared with the curve calculated according to Eq.(6) with²⁴ $n_c = n_{c2}$ and $g = 1.4g_0 = 2.8$. One can see that (i) in full agreement with Eq.960, the experimental curves in the region where they overlap do scale with the magnitude of the magnetic field; (ii) the dependence given by Eq.(6) qualitatively agrees with the experimental results; and (iii) there is a noticeable quantitative disagreement. Especially troublesome is the discrepancy in the density range $2 \times 10^{11} \text{ cm}^{-2} < n_s < 4 \times 10^{11} \text{ cm}^{-2}$, where it is clearly larger than the possible error and cannot be attributed to the finiteness of the temperature or the inhomogeneity of the sample. Most probably, this discrepancy results from the use of the parameters obtained for electrons at the chemical potential level to describe electrons within the Fermi distribution.

Next, let us discuss the measurements of the field of complete spin polarization B_p for a magnetic field oriented parallel to the interface. The corresponding experimental data are shown in Fig.(4). For comparison, the results of independent measurements are shown by lines. The thin solid line passing slightly above the experimental points is obtained using

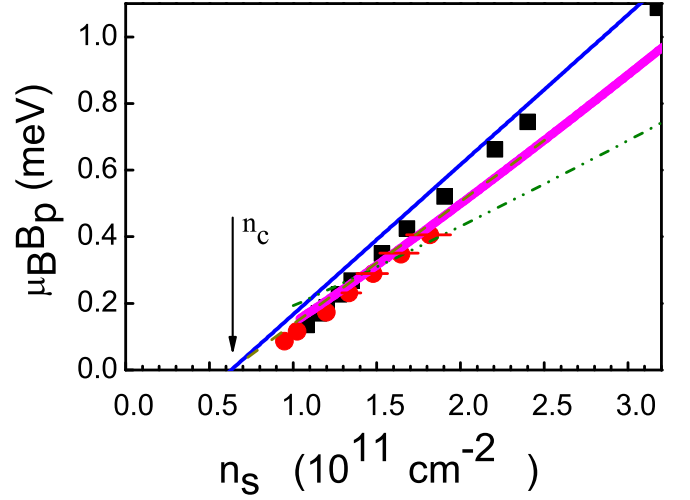


FIG. 4: (Color online) Field corresponding to the complete spin polarization of electrons versus their density. The thin line shows the result of calculations using the fitting line drawn through the experimental points in Fig.(1) for $g = 1.4g_0$; the thick line shows the expected field of complete spin polarization calculated for the parameters at the chemical potential level [4, 10]. Squares and circles correspond to the measurements of the magnetoresistance saturation field [24] and the results from [23], respectively. The dash-dotted line is drawn according to the calculations of [20] for an ideal electron system using the experimental Lande factor.

the interpolation of the data from Ref.¹⁴ and the Lande factor $g = 1.4g_0$ according to the formula

$$\mu_B B_p = \frac{n_s \pi \hbar^2}{m g}, \quad (7)$$

which corresponds to the model of free electrons with the renormalized mass and Lande factor. The thick solid line is obtained from independent experiments^{4,10}, where the product gm is described by the expression

$$gm = g_0 m_b (1 + 0.21 r_s + 0.003 r_s^3 + 0.0000045 r_s^6). \quad (8)$$

One can see that both the experimental points and the two solid lines fall on straight lines with somewhat differing slopes at electron densities above 10^{11} cm^{-2} . The difference in the slopes does not exceed the systematic experimental errors, and the extrapolation of both fitting lines to zero value of the field B_p yields the same critical density $n_c = 0.63 \times 10^{11} \text{ cm}^{-2}$. This value is lower than that obtained by the extrapolation of the straight line drawn through the experimental points, which is probably caused by the abovementioned overestimation of the energy required for the complete spin polarization of the electron system.

The quantum Monte Carlo calculation of the complete spin polarization field²⁰ also yields a curve close to a straight line in the region of interest on the (n_s, B_p) plane (see Fig.4). However, its slope is noticeably smaller than the one obtained experimentally. According to Ref.²⁰, the dependence of the complete spin polarization field B_p on the electron density n_s

in an electron system with disorder is qualitatively different: B_p becomes zero for a finite value of n_s . This behavior resembles that observed experimentally. Nevertheless, even in this case, the calculation noticeably underestimates the energy required for complete spin polarization for electron densities exceeding $2 * 10^{11} \text{cm}^{-2}$. However, if the Lande factor determined for electrons at the chemical potential level does not describe electrons within the Fermi distribution and is considered as an additional fitting parameter, a calculation²⁰ using these two parameters (the degree of disorder and the Lande factor g) can fit the experimental data in Fig.4 quite satisfactorily.

The transition of an electron system subjected to a field B_p to a completely spin polarized state must be accompanied by an abrupt change in the thermodynamic density of states and, consequently, in the capacitance of the MOSFET structure. An example of a corresponding experimental plot is shown in Fig.2.

Using Eq.(6), it is easy to calculate the chemical potential of a partially polarized electron system in a magnetic field $B < B_p$:

$$\mu(B, n_s) = \mu(0, n_n) + \left(\frac{\mu_B g B}{2}\right)^2 \frac{m_b}{\pi \hbar^2} \frac{n_c}{(n_s - n_c)^2}, \quad (9)$$

where $\mu(0, n_n)$ is given by Eq.(3). Then, the inverse of the thermodynamic density of states equals

$$\frac{\partial \mu}{\partial n_s} = \frac{\pi \hbar^2}{2m_b} - \frac{(\mu_B g B)^2 m_b n_c}{2\pi \hbar^2 (n_s - n_c)^3}. \quad (10)$$

It varies most pronouncedly in the vicinity of the transition to the spin polarized state:

$$\frac{\partial \mu}{\partial n_s}(B_p) = \frac{\pi \hbar^2}{2m_b} \left(1 - \frac{n_c}{(n_s(B_p) - n_c)}\right). \quad (11)$$

The second term in the braces in Eq. (11) is not small, especially for $B_p \rightarrow 0$. Nevertheless, no experimental manifestations of this term have been observed. Indeed, according to Eq. (11), one would expect the occurrence of distinctly nonzero values of $|\Delta C/C|$ for densities above the observed jump in the capacitance. This behavior is seen neither in Fig.2 nor in any of the experimental curves in²³.

Such a significant discrepancy arises because the quantity μ used in Eqs.(5,6,9,10,11) is the chemical potential measured with respect to the free electron level, while screening (and, thus, the capacitance) is determined by the difference between the chemical potential and the energy at the bottom of the two-dimensional electron subband. In experiments where the shift of the subband bottom caused by external factors is not important, all above expressions are valid. The second term in Eq. (9) equals the shift of the subband bottom, which can be easily seen by considering the limiting case $B \rightarrow B_p$. This second term has to be omitted in the subsequent formulas that describe screening. As a result, it should be expected that the absolute value of the capacitance jump in the spin polarizing

field will coincide with the horizontal line in Fig.2. Actually, according to the figure, this jump proves to be 25% smaller.

Frequently, the two-dimensional electron system in *SiMOSFETs* is described in terms of another approach based on the Landau theory of Fermi liquids. On one hand, this requires the introduction of a larger number of parameters (amplitudes F_0^s, F_0^a, F_1^s instead of m and g) to be determined from the experiment; on the other hand, this makes it possible to deal only with quasiparticles within a narrow energy range in the vicinity of the chemical potential level.

Since the effective mass that determines the compressibility and thermodynamic density of states of an electron system depends on two amplitudes F_0^s and F_1^s as

$$m_{com} = \frac{m}{1 + F_0^s} = m_b \frac{1 + F_1^s}{1 + F_0^s}, \quad (12)$$

the weak dependence of the capacitance jump on the electron density (see Fig.2) implies²⁶ that $F_0^s \simeq F_1^s$.

It proves that the Fermi liquid parameter most sensitive to the interaction is F_1^s . According to Eqs.(2) and (12), F_1^s can be expressed in the investigated range of electron densities as

$$F_1^s = \frac{r_{sc}^2}{(r_{sc}^2 - r_s^2)}, \quad (13)$$

and is larger than 2 for an electron density of 10^{11}cm^{-2} , which corresponds to $r_s \simeq 8$.

It is no surprise that the functional dependences of F_0^s and F_1^s are the same, because both amplitudes are harmonics of the same function $F_{\mathbf{k}, \mathbf{k}'}$, and the coincidence of their magnitudes within the experimental error means that the dependence of $F_{\mathbf{k}, \mathbf{k}'}$ on the angle between vectors \mathbf{k} and \mathbf{k}' is weak.

The parameter investigated in most detail (see¹⁰) is F_0^a , because it is expected that it can be determined from two different experiments, i.e., from the measured values of the Lande factor and from the linear temperature dependence of the elastic relaxation time²⁷. The results obtained demonstrate within the actual experimental accuracy that F_0^a depends weakly on the electron density in the range from $1.9 * 10^{11} \text{cm}^{-2}$ to about $1 * 10^{12} \text{cm}^{-2}$. At lower electron densities, a considerable increase in $|F_0^a|$ takes place, in fair agreement with the result of Ref.²⁶.

Thus, any one of the methods used for experimental data treatment leads to qualitatively coinciding results for F_0^a . One can hardly expect better agreement because of both limited experimental accuracy and limited applicability of the model used in Ref.²⁷ and later publications. For example, the theory does not take into account in any way that the scattering potential in Si MOSFETs changes radically in the range of electron densities under consideration. For the lowest densities, it is the screened Coulomb potential; as the density increases, it changes over to interface roughness scattering. Possibly, the experimental results obtained in Ref.²⁸, which differ somewhat from those considered above, follow from the change in the density corresponding to the transition between different scattering potentials.

In conclusion, let us once again stress the striking fact that a system of strongly interacting two-dimensional electrons can

be described with good accuracy in terms of a gas of non-interacting electrons with the renormalized mass and Lande factor, and this description demonstrates its predictive power. Hopes for further progress in the experimental investigation of the two-dimensional electron system in silicon MOSFETs in the region of low densities and high mobilities are associated with precision measurements of the thermodynamic density

of states.

I am grateful to S.V. Kravchenko, V.M. Pudalov, and A.A. Shashkin for useful discussions. This study was supported by the Russian Foundation for Basic Research (project nos. 13-02-00095 and 13-02- 12127) and the Russian Academy of Sciences.

-
- ¹ T. Ando, A. B. Fowler, and F. Stern, Rev. Mod. Phys. **54**, 437 (1982)
 - ² A. Mokashi, S. Li, Bo Wen, S. V. Kravchenko, A. A. Shashkin, V. T. Dolgoplov, M. P. Sarachik Phys. Rev. Lett. **109**, 096405 (2012)
 - ³ A.Yu. Kuntsevich, L.A. Morgun, V.M. Pudalov Phys. Rev. **B 87**, 205406 (2013)
 - ⁴ V. M. Pudalov, M. E. Gershenson, H. Kojima Phys. Rev. **B 90**, 075147 (2014)
 - ⁵ S.V. Kravchenko, M.P Sarachik Reports on Progress in Physics **67**, 1 (2004)
 - ⁶ A.A. Shashkin Physics-USpekhi **48**, 129 (2005)
 - ⁷ Knyazev D.A., Omel'yanovskii O.E., Pudalov V.M., Burmistrov I.S., Phys. Rev. Lett. **100**, 046405 (2008).
 - ⁸ S.V. Kravchenko, M.P Sarachik International Journal of Modern Physics **B 24**, 1640 (2010)
 - ⁹ Knyazev D. A., Omelyanovskii O. E., Pudalov, V. M. Solid State Communications **144**, 518 (2007)
 - ¹⁰ Klimov N. N., Knyazev D. A., Omel'yanovskii O. E., Pudalov V.M., Kojima H., Gershenson M.E. Phys. Rev. **B 78**, 195308 (2008).
 - ¹¹ Shashkin A. A., Kapustin A. A., Deviatov E. V., Dolgoplov V.T., Kvon Z.D., Kravchenko S.V. Journal of Physics A-Mathematical and Theoretical **42**, 214010 (2009)
 - ¹² A.A. Shashkin, V.T. Dolgoplov, J.W. Clark, V.R. Shaginyan, M.V. Zverev, V.A. Khodel Puys. Rev. Lett., **112**, 186402 (2014).
 - ¹³ V. M. Pudalov, M. E. Gershenson, H. Kojima, N. Butch, E.M. Dizhur, G. Brunthaler, A. Prinz and G. Bauer, Phys. Rev. Lett., **88**, 196404 (2002)
 - ¹⁴ A.A. Shashkin, Maryam Rahimi, S. Anissimova, S.V. Kravchenko, V.T. Dolgoplov, T.M. Klapwijk Phys. Rev. Lett. **91**, 046403 (2003)
 - ¹⁵ V.T. Dolgoplov JETP Letters **76**, 377 (2002).
 - ¹⁶ V.T. Dolgoplov, A.A. Shashkin **95**, 648 (2011)
 - ¹⁷ V. Dobrosavljevic, in 'Conductor Insulator Quantum Phase Transitions', edited by V. Dobrosavljevic, N. Trivedi, and J. M. Valles Jr. (Oxford University Press, 2012).
 - ¹⁸ M.Ya. Amusia, K.G. Popov, V.R. Shaginyan, V.A. Stephanovich, Theory of Heavy Fermion Compounds, Springer (2014)
 - ¹⁹ Suhas Gangadharaiah and Dmitrii L. Maslov Phys. Rev. Lett., **95**, 186801 (2005).
 - ²⁰ Geneviève Fleury and Xavier Waintal Phys. Rev. **B 81**, 165117 (2010)
 - ²¹ V. S. Khrapai, A. A. Shashkin, V. T. Dolgoplov Phys. Rev. **B 67**, 113305 (2003)
 - ²² O. Prus, Y. Yaish, M. Reznikov, U. Sivan, V. Pudalov Phys. Rev. **B 67**, 205407 (2003)
 - ²³ A. A. Shashkin, S. Anissimova, M. R. Sakr, S. V. Kravchenko, V. T. Dolgoplov, T. M. Klapwijk Phys. Rev. Lett. **96**, 036403 (2006)
 - ²⁴ A. A. Shashkin, S. V. Kravchenko, V. T. Dolgoplov, T. M. Klapwijk Phys. Rev. **B 66**, 073303 (2002)
 - ²⁵ To avoid misunderstanding, the expansion in the Landau amplitudes for the two-dimensional case used below has the form $F_{\mathbf{k},\mathbf{k}'}^{s,a} = F_0^{s,a} + 2\sum_{n=1}^{\infty} F_n^{s,a} \cos(n[\theta - \theta'])$.
 - ²⁶ A. Gold, V.T. Dolgoplov **86**, 687 (2007)
 - ²⁷ G. Zala, B.N. Narozhny, I.L. Aleiner Phys. Rev. **B 64**, 214204 (2001)
 - ²⁸ S.A. Vitkalov, K. James, B.N. Narozhny, M.P. Sarachik, and T.M. Klapwijk, Phys. Rev. **B 67**, 113310 (2003).